ARCHIVE OF MECHANICAL ENGINEERING

DOI: 10.24425/ame.2022.143095 2022, Vol. 69, No. 4, pp. 571–594

Jacek BUŚKIEWICZ [1]

Kinematic synthesis of the mechanism for static balancing of an input torque in three positions

Received 23 February 2022, **Revised** 28 June 2022, **Accepted** 20 September 2022, **Published online** 21 November 2022

Keywords: mechanism synthesis, machine design, discrete balancing, torque balancing

The aim of this work is to design the links-spring mechanism for balancing, in the three positions of the operating range, a rotary disc subjected to a torque. An energy-related approach towards the conditions of the mechanical system balance for a discrete number of positions leads to the formulation of a task of searching for a four-bar linkage which guides a coupler point through the prescribed positions, where, at the same time, geometrical conditions (specifying the spring tension) and kinematic conditions (defining the radial component of the tension change rate) are satisfied. The finitely and infinitesimally separated position synthesis is considered, however, only a component of the coupler point velocity is essential. A general method was proposed for determining the four-bar mechanism geometry. Mechanism inversion was applied in order to reduce the number of designed variables and simplify the solution method. The system of complex algebraic equations defines the problem. Linear, symbolic transformations and a systematic search technique are utilized to find multiple local optimal solutions. The problem is solved using Mathematica software.

1. Introduction

The balancing of a spatial and planar linkage-spring system is of crucial importance in reducing the energy consumed by machines while performing prescribed operating functions The balancing in a finite (discrete) number of positions is a particular kind of linkage balancing. The aim of this work is to design (to select the dimensions and mechanical parameters) the links-spring system for balancing, in the three positions of the operating range, a rotary disc loaded with a torque. An energy-related approach towards the conditions of the mechanical system balance for a discreet number of positions leads to the formulation of a task of searching

✉ Jacek Buśkiewicz, e-mail: jacek.buskiewicz@put.poznan.pl

[1] Poznan University of Technology, Poznan, Poland. ORCID: 0000-0002-8110-1473

for a mechanism which guides an operating element through the prescribed positions, where, at the same time, geometrical conditions (specifying the spring tension) and kinematic conditions (defining the radial component of the tension change velocity) must be satisfied. In other words, the finitely and infinitesimally separated positions synthesis is considered. In this specific task, the rigid body motion is represented by the three finitely separated positions associated with three infinitesimally separated positions. However, a velocity condition (related to the infinitesimally separated positions) is defined in a slightly different way as only a component of the coupler point velocity is essential. The overview of the literature indicates some drawbacks in the research on the methods enabling the designing of mechanisms which ensure balance in the finite discrete positions.

The present paper investigates a mechanism for balancing an external load. The linkage weight is not considered, and the external load is reduced to the torque subjected to a member of the linkage. Most of the papers, however, deal with the balancing of the linkages weights by means of counterweights, both zero-free-length and non-zero-free-length springs as well as auxiliary links, cables and pulleys, cams, gear trains and devices compiling a few solutions [1]. The force/torque balancing is closely related with the modelling of force/torque generators [1–7].

The first observation arising from the literature review is that balancing of linkages requires additional solutions that are frequently complex with regard to the manufacturing issues, e.g., cam mechanisms, gear trains, etc. The four-bar linkage has an advantage in that the kinematic structure and manufacturing process are simple. In the recent studies, we can find four-bar linkages that are mechanical parts of statically balanced mechanisms [4, 8–13]. However, In order to produce the gravity balanced planar mechanism, a four-bar linkage frequently requires either additional linkages or nonlinear springs [8, 10]. In paper [4] the method used for the design of statically balanced mechanisms is exemplified by the static balancing of four-bar linkages with torsion springs. The use of zero-free-length springs is not required and the linear spring can be used in either a tensile or compressive configuration.

The second comment is that these studies deal with balancing either over the full motion range of the system or over the finite continual range of motion. The problem of discrete balancing at chosen positions is of less interest. The problem is trivial when balancing at one position is considered, and one can still expect no significant difficulty when balancing at two positions. With regard to the key problem of our paper, one can focus attention on paper [14]. This study deals with discrete balancing, where balancing is ensured in 12 distinct angular positions of a robot arm.

We may also notice that the methods worked out to synthesize statically balanced mechanisms are mainly based on the knowledge and experience of researchers. The geometry of the mechanism is proposed a priori, frequently it is a modification or development of existing, well-known mechanisms, and then the dimensions are determined from the equations expressing the equilibrium conditions.

The general synthesis methods only are worked out and applied to basic linkages, when other approaches fail to find the optimal parameters of a balanced system. When balancing at three or more positions is required with a non-symmetrical distribution of the balancing positions, the problem becomes difficult to solve.

The fact that the majority of geometric synthesis methods have been worked out for a four-bar linkage encourages ones to apply this linkage to produce balanced systems. Countless synthesis methods have been worked out. Among them, one can distinguish the synthesis methods for solving the problems for which there exist mechanisms that accurately realize the imposed conditions, i.e., the requirement for a coupler point to pass through a relatively small number of positions [15–18]. The so-called solution region synthesis methodology for the eight-precision-point path synthesis of planar four-bar mechanisms is presented in [19]. The problem of finding all four-bar linkages whose coupler curve passes through nine prescribed points is undertaken in [20] using a combination of classical elimination, multihomogeneous variables and numerical polynomial continuation.

Nevertheless, it is the problem studied in papers [21–23] that is the most similar to the problem formulated in the present paper. Slightly simpler, but analytically solvable, tasks are formulated there. A synthesis method with both coupler trajectories and velocities (a bi-objective problem) was solved in [21]. An analytical solution using this method was presented for straight line path generation [22]. Having given three pairs of coincident curve points, a four-bar linkage was synthesized. The constraints include two separate position constraints and one velocity constraint. Three four-bar linkages, with two symmetrical coupler curves and one asymmetrical curve, were synthesized simultaneously for one given independent design parameter. The synthesis of planar linkage mechanisms with approximate velocity constraints is presented in [23]. Two precision positions with velocity prescribed at one of the positions allows one to formulate the first closed-form complex-number dyad solution to the ground pivot specification problem. On the basis of this solution, approximate velocity constraints are added to design methods for two exact positions and an unlimited number of approximate positions. The increase in the number of velocity conditions requires a numerical technique for finding approximate solutions. The mathematical complexity of the mechanism synthesis problems grows with the number of precision points, and the equations cannot be effectively solved using an analytical approach. The synthesis problem with more than nine precision points can be expressed by approximate solutions obtained via optimization methods. Work [24] summarizes the developments made in quantitative four-bar path and function generation. The up-to-date achievements in computing hardware and software allow for the efficient solving of many geometric problems. The full rotation conditions, circuit and branches defects avoidance, and the correct coupler points order are usually controlled by synthesis algorithms. A detailed review on the mechanism synthesis methods can be concluded that the studies focus on the developing geometric synthesis methods which contain no additional kinematic constraints. The synthesis problem expressed simultaneously by

kinematic and geometric conditions at selected instants is not widely reported. The reason is that the problem is complex, and the solutions for a particular mechanism satisfying two geometric and only one kinematic condition were found. More complex problems have to be solved numerically. In point of fact, the formulation of the purely theoretical problem gives rise to uncertainty about whether the solution method used is effective in a particular practical problem in terms of the necessity of satisfying many extra constraints of a technical nature, e.g., the housing size.

To summarize, the design of the mechanical systems subjected to external loads and balanced in a discrete number of positions is a challenging task. There are no techniques for the determination of the geometric parameters of the prescribed mechanisms for a wide range of input data. The present paper utilizes approaches worked out in kinematics and synthesis of mechanisms for this purpose. In order to balance the disc subjected to a torque in three arbitrarily prescribed positions, the mechanical system composed of a four-bar linkage and spring is proposed and the system parameters have to be determined. On the basis of the equilibrium equations, a new combined finitely-infinitesimally separated positions synthesis problem was formulated and the solution method was worked out. The kinematic inversion simplifies the system description and enables formulation of the problem by means of a reduced number of design parameters. The reduced number of optimized parameters allows for searching for the optimal solutions by searching through the design space and therefore a heuristic algorithm is not required.

2. Problem formulation

Let us suppose that a horizontal disc with the vertical axis of rotation O_1 is subjected to resistance torque M_E. Let the torque act clockwise. The objective is to design such a mechanical system – with the structure as simple as possible – based on revolute pairs and a spring, that the disc is balanced in three prescribed angular positions. The synthesized mechanism couples the disc's angular position and the spring tension in order that the equilibrium conditions are satisfied (Fig. 1).

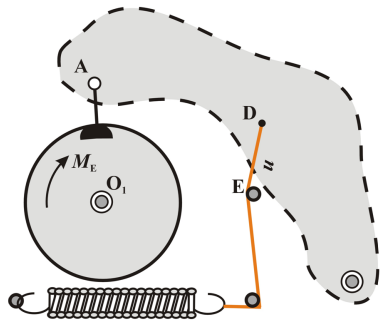

Fig. 1. The scheme of the system for the purpose of structural synthesis

Let the disc be rigidly connected to the active link of the mechanism. A spring-coupler point D regulates the spring extension. Let ground point E be attached to the frame and let the distance |DE| be equal to the spring extension. The force for the free length spring is 0. The system operates in the horizontal plane and the forces of gravity are taken into account. Assuming that moments of the friction forces in the kinematic pairs are neglected, the problem consists in determining the dimensions of the mechanism (which regulates the spring extension), for which the system is in balance for a prescribed function of the torque in the three selected positions expressed by angular positions of the disc. Let the torque have a constant value, though the assumption of a constant torque value is not required, and in general the method is applicable for a varying torque.

A separate issue, not discussed thoroughly in this paper, is how to ensure in technical implementation that the distance |DE| is equal to the spring extension. Let us mention that an additional part has to be mounted at point E. It may be a rotating pin designed to minimise the deviation of the actual distance |DE| from the theoretical one. Other solution is to insert the spring inside a revolute tube pivoted at point E.

We carry out analytical considerations to determine the equilibrium equations in the prescribed positions of the system. The constraints being ideal, the sum of the elementary work $\mathrm{d}W$ done by the torque and the elementary work of the spring force (the change in the spring potential energy $\mathrm{d}U$) in the vicinity of the equilibrium position (balance position) is equal to 0 (or in other words, the sum of the potential energy and the work of non-potential forces is locally constant). Let u stand for spring extension. Then

$$\mathrm{d}W = -M_{\mathrm{E}}\,\mathrm{d}\theta_1 - ku\,\mathrm{d}u = 0. \tag{1}$$

To derive the formula for spring extension, one can integrate Eq. (1) over the disc rotation from the initial angular position θ_1 by $\Delta\theta_1$. The spring extension will change from the initial (maximum) one, denoted as $u_{\max} = u(\theta_1)$, to a certain extension u. The change in the spring potential energy makes up for the work of the resistance torque.

$$-\int_{\theta_1}^{\theta_1+\Delta\theta_1} M_{\mathrm{E}}\,\mathrm{d}\theta_1 = \int_{u_{\max}}^{u} ku\,\mathrm{d}u = -M_{\mathrm{E}}\Delta\theta_1 = \left(\frac{1}{2}ku^2 - \frac{1}{2}ku_{\max}^2\right). \tag{2}$$

We obtain from Eq. (2) the formula for |DE| – that is, for the spring extension required to maintain equilibrium:

$$u = \sqrt{u_{\max}^2 - \frac{2M_{\mathrm{E}}}{k}\Delta\theta_1}\,, \tag{3}$$

where $\Delta\theta_1$ is the input link rotation measured from the initial position. The equality $|\mathrm{DE}| = u$ suffices to express equilibrium, when equilibrium for a continuous interval

of the system positions is considered, and the discretisation of the independent variable (input link angular position) is sufficiently dense. Notice that when a low discrete number of balance positions is considered, the formula for spring extension (3) itself does not suffice to ensure the equilibrium. The other condition results directly from Eq. (1):

$$\mathrm{d}W = -M_{\mathrm{E}}\,\mathrm{d}\theta_1 - ku\,\mathrm{d}u = \left(-M_{\mathrm{E}} - ku\frac{\mathrm{d}u}{\mathrm{d}\theta_1}\right)\mathrm{d}\theta_1 = 0, \tag{4}$$

and relates the rate of change of the spring extension with respect to the input link angle with the input torque, spring stiffness and spring extension:

$$\frac{\mathrm{d}u}{\mathrm{d}\theta_1} = \frac{-M_{\mathrm{E}}}{ku}\,. \tag{5}$$

On the basis of the above reasoning, one can formulate the task of designing a mechanism for torque balancing as a specific problem of mechanism geometric-kinematic synthesis:

Determine the location of the frame point (denoted as E) *and the mechanism dimensions with the position of such a point* (denoted as D) *that the distance* |DE| *and the radial component of the velocity of point* D *with respect to point* E *take values expressed by Eqs. (3) and (5) in the prescribed input link positions.*

We determine the mechanism that ensures the equilibrium for three angular positions of the disc (input link) defined by angles θ_{11}, θ_{12} and θ_{13}, which can equivalently be described by two angular increments $\Delta\theta_{12} = \theta_{12} - \theta_{11}$, $\Delta\theta_{13} = \theta_{13} - \theta_{11}$. Then, the problem can be graphically illustrated as shown in Fig. 2. The position of the disc at instant i – $\mathrm{O_1A}_i$ is associated with the adequate i-th position of point D, distance u_i and radial velocity component $v_i = \dot{u}_i = |\dot{\mathrm{ED}}_i|$. The tangential velocity component is drawn as a dotted line. The geometric (3) and kinematic (5) conditions for a single equilibrium position may be also interpreted as follows.

The locations of points D and E are not known. For a chosen equilibrium position the condition for the spring extension defines the circle centred at D and of radius u, and the condition for infinitesimal displacement du (derivative of u) allows us to locate the point E on this circle. The circle centred at $\mathrm{D_1}$ in Fig. 2 illustrates the case for the first position $u = u_1$. The problem was break down into two sub-problems geometric (for u) and kinematic (for derivative of u) in order to utilize methods used in mechanism analysis.

We postulate the four-bar linkage (Fig. 3) composed of input link $\mathrm{O_1A}$ rigidly connected to the disc, output rotating link $\mathrm{O_2B}$ and coupler ADB. The conditions of static balancing of four-bar linkage in a single position are formulated in paper [4]. The difference is that in [4] the torsion spring are attached at the linkage's revolute joints and the continuous range of motion is considered. In the equilibrium a negative stiffness function created by a nonzero-free-length spring cancels the

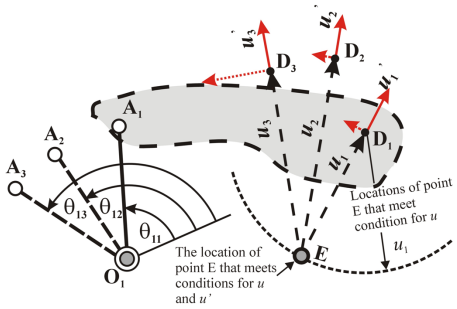

Fig. 2. Graphical illustration of the synthesis problem

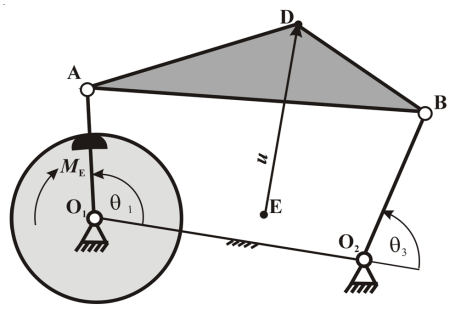

Fig. 3. The scheme of the four-bar linkage with the loaded disc

positive stiffness function of torsion springs attached at the revolute joints. The type of stability is specified by analyzing the relation between curvature radiuses of the spring-coupler point and spring's equipotential circle.

2.1. Solution method

The methods developed in mechanism synthesis can be divided into two categories. The first defines the problem by means of all the design parameters that fully describe the geometry of the mechanism, and focuses on developing and enhancing optimisation algorithms. The other branch involves methods that aim at decreasing the number of design parameters by using kinematic inversion, special error functions, etc. These methods are frequently referred to as two-phase mechanism synthesis. The method applied in this paper belongs to this category.

We apply complex numbers to describe the mechanism positions. The mathematical formulae of the closed loop O_1ADEO_1 for the three prescribed positions is not profitable. The reason is the variation of the angular orientation of ED, which results in the necessity of introducing the angle that describes the orientation of segment ED. This angle, useless for further analysis, makes mathematical equations more complex. Moreover, the derivative of the closed loop equations contains Cartesian components of point D velocity, whereas the radial component only is important. Taking into account these observations, we pursue the simplification of the mathematical form of the closed loop equations. The concept of kinematic inversion is used, and as a consequence segment ED becomes the immoveable reference link. Frame O_1O_2 is fixed in the four-bar linkage, whereas in the auxiliary mechanism (obtained as a result of kinematic inversion) the motion will be described with respect to the axis passing through points E and D. After kinematic inversion, axis ED is the axis of the guide link for slider D. The scheme of the auxiliary mechanism is shown in Fig. 4. The mechanism is driven by the linear motion of slider D along guide link DE so that $|DE| = u$. Link ABD is connected to slider D and to links O_1A and O_2B using revolute joints. Links O_1A and O_2B create revolute pairs with link EO_1O_2, the one that is pivoted to the frame at revolute joint E. We

utilize also Fig. 5 for the purposes of geometric analysis. The kinematic inversion changes the structure of the mechanism. The four-bar linkage has 3 moveable links and 4 revolute kinematic pairs, whereas the auxiliary mechanism has 5 links and 7 kinematic pairs (6 revolute and 1 prismatic). Though, the degree of mobility for both mechanisms equals 1.

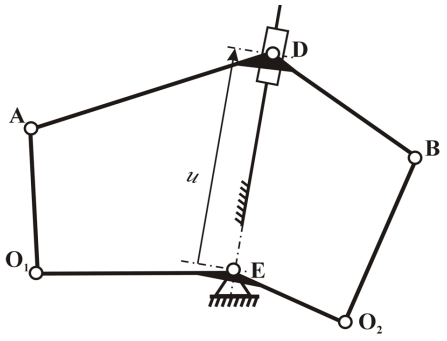

Fig. 4. The scheme of the auxiliary mechanism

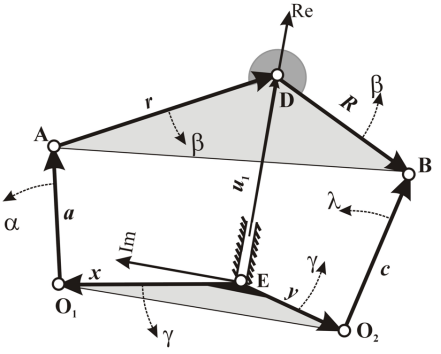

Fig. 5. The angles measured from the first equilibrium position of the mechanism

The reference position is the mechanism position associated with the first equilibrium position described by complex numbers $\boldsymbol{a}, \boldsymbol{x}, \boldsymbol{y}, \boldsymbol{r}, \boldsymbol{R}$ and $\boldsymbol{c}$. The following angles are introduced, and shown in Fig. 5:

- α – angular position of link O_1A measured from the first position of link O_1A (the first position of link O_1A is described by complex number $\boldsymbol{a}$),
- γ – angular position of arms EO_1 and EO_2 of link O_1EO_2 measured from the first position of EO_1 and EO_2 described by complex numbers $\boldsymbol{x}$ and $\boldsymbol{y}$, respectively,
- β – angular position of arms AD and DB of link ADB measured from the first position of AD and DB described by complex numbers $\boldsymbol{r}$ and $\boldsymbol{R}$, respectively,
- λ – angular position of link O_2B measured from the first position of O_2B described by complex number $\boldsymbol{c}$.

Let axis x(Re) be oriented along ED, and axis y(Im) be perpendicular to x. We consider three mechanism positions with the spring extensions (|DE| distances) equal to:

a)
$$u_1 = \sqrt{u_{\max}^2 - \frac{2M_E}{k}0} = u_{\max}\,, \tag{6}$$

for the rotation of O_1A about O_1O_2 (in the four-bar linkage – Fig. 3) by angle $\Delta\theta_{11} = \theta_{11} - \theta_{11} = 0$;

b)
$$u_2 = \sqrt{u_{\max}^2 - \frac{2M_E}{k}\Delta\theta_{12}}\,, \tag{7}$$

where $\Delta\theta_{12} = \theta_{12} - \theta_{11}$;

c)
$$u_3 = \sqrt{u_{\max}^2 - \frac{2M_E}{k}\Delta\theta_{13}} = u_{\min}\,, \tag{8}$$

where $\Delta\theta_{13} = \theta_{13} - \theta_{11}$.

Eq. (8) relates the minimum and maximum spring extensions. The first position described by $\boldsymbol{a}$, $\boldsymbol{x}$, $\boldsymbol{y}$, $\boldsymbol{r}$, $\boldsymbol{R}$ and $\boldsymbol{c}$ corresponds to the solution for $u = u_1$.

The angle of rotation of O_1A must be expressed by means of angle θ_1, which in the four-bar linkage (Fig. 3) is measured from O_1O_2. The closed loop equations will be formulated for the auxiliary mechanism shown in Fig. 4. Then, the angular position of link O_1A with respect to O_1E in the auxiliary mechanism must be computed and expressed by means of θ_1 (or $\Delta\theta_1$), which is the independent variable of u and derivatives of u. We introduce angle α^* between O_1A and O_1E. This angle is the sum of θ_1 and a constant value denoted as C and equal to the angle at O_1 in triangle EO_1O_2 with the appropriate sign. The change in θ_1 equals the change in α^*. Angle γ^* is measured between ED and O_1E. We compute the angle between O_1A and an arbitrary fixed immovable axis – let us take the axis parallel to ED, which has a fixed angular orientation. As shown in Fig. 6, this angle is equal to $\alpha^* + \gamma^* - \pi$. Hence, if O_1E rotates by γ with respect to its first position, and O_1A rotates by $\Delta\theta_1$ with respect to O_1E, then O_1A will rotate by $\alpha = \Delta\theta_1 + \gamma$ with respect to the fixed axis, and simultaneously with respect to its first position defined by $\boldsymbol{a}$.

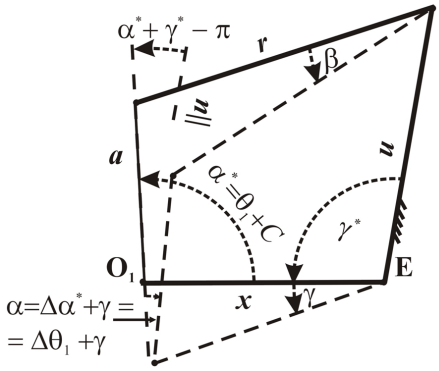

Fig. 6. Geometric illustration for determining angle α

Let us write the closed loop equations using the complex number notation ($i = \sqrt{-1}$) for the first equilibrium position, shown in Fig. 5:

$$\boldsymbol{x} + \boldsymbol{a} + \boldsymbol{r} - u_1 = 0, \tag{9}$$

for the second one obtained after rotation of O_1A with respect to O_1E by $\Delta\theta_{12}$:

$$\boldsymbol{x}e^{i\gamma_2} + \boldsymbol{a}e^{i(\Delta\theta_{12}+\gamma_2)} + \boldsymbol{r}e^{i\beta_2} - u_2 = 0, \tag{10}$$

and the third one obtained after rotation of O_1A with respect to O_1E by $\Delta\theta_{13}$:

$$\boldsymbol{x}e^{i\gamma_3} + \boldsymbol{a}e^{i(\Delta\theta_{13}+\gamma_3)} + \boldsymbol{r}e^{i\beta_3} - u_3 = 0. \tag{11}$$

For the first equilibrium position we have $\gamma_1 = \beta_1 = \lambda_1 = 0$. For the subsequent positions the links rotate by β_j, γ_j, λ_j. Distance u is expressed by means of angle θ_1, and we differentiate Eqs. (9)–(11) with respect to θ_1. Measured from the first equilibrium position, angular increment $\Delta\theta_1$ differs from angle θ_1 (measured from O_1O_2) by a constant value, then $\mathrm{d}(\Delta\theta_1) = \mathrm{d}\theta_1$. If the general formula for the closed loop equation in the i-th position is written as follows:

$$\boldsymbol{x}e^{i\gamma_j} + \boldsymbol{a}e^{i(\Delta\theta_{1j}+\gamma_j)} + \boldsymbol{r}e^{i\beta_j} - u_j = 0, \quad j = 1, 2, 3, \tag{12}$$

the adequate derivative can be written in the form:

$$\boldsymbol{x}\gamma_j' ie^{-i\gamma_j} + \boldsymbol{a}\left(1 + \gamma_j'\right) ie^{i(\Delta\theta_{1j}+\gamma_j)} + \boldsymbol{r}\beta_j' ie^{i\beta_j} - v_j = 0, \quad j = 1, 2, 3, \tag{13}$$

where: $\beta_j' = \dfrac{\mathrm{d}\beta}{\mathrm{d}\theta_1}\left(\Delta\theta_{1j}\right)$, $\gamma_j' = \dfrac{\mathrm{d}\gamma}{\mathrm{d}\theta_1}\left(\Delta\theta_{1j}\right)$.

Similarly, the equations for loop $EDBO_2$ are written. We note that the joints A, D and B lie on the same rigid link as the joints O_1, E and O_2 do. On the basis of this observation, we introduce only one extra angle λ to describe the angular displacement of link O_2B with respect to the position occupied by this link in the first equilibrium position.

$$\boldsymbol{y}e^{i\gamma_j} + \boldsymbol{c}e^{i\lambda_j} - \boldsymbol{R}e^{i\beta_j} - u_j = 0, \quad j = 1, 2, 3. \tag{14}$$

The general form of the derivatives can be written in the form:

$$\boldsymbol{y}\gamma_j' ie^{i\gamma_i} + \boldsymbol{c}\lambda_j' ie^{i\lambda_j} - \boldsymbol{R}\beta_j' ie^{i\beta_j} - v_j = 0, \quad j = 1, 2, 3, \tag{15}$$

where $\lambda_j' = \dfrac{\mathrm{d}\lambda}{\mathrm{d}\theta_1}\left(\Delta\theta_{1j}\right)$.

Let us derive the general correspondence between the number of prescribed geometric and kinematic conditions and the number of the unknown parameters. Let m denote the number of geometric equations (u_j), n stand for the number of kinematic equations (v_j). There is a complex (vector) equation for each u_j as well as for each v_j. The total number of equations is 2 (number of the closed loops) $\times$2 (real and imaginary part of a complex equation) $\times(m+n) = 4(m+n)$. The unknowns are: 12 components of 6 complex numbers $\boldsymbol{a}$, $\boldsymbol{x}$, $\boldsymbol{r}$, $\boldsymbol{c}$, $\boldsymbol{y}$, $\boldsymbol{R}$, $3n$ angular velocities γ_j', β_j', λ_j', $j = 1, \ldots, n$ and $3m$ angles α_j, β_j, λ_j, $j = 1, \ldots, m$, where $\alpha_1 = 0$, $\beta_1 = 0$, and $\lambda_1 = 0$. Then, the total number of variables equals to $12+3n+3(m-1)$. By equalling the numbers of equations and parameters, one obtains that there are no free choices when $m + n = 9$. When $m = n = 3$, as is the case herein, three design parameters can be prescribed. The classical path synthesis problem without

timing for the four-bar linkage has the finite number of the solutions for up to nine prescribed precision points [20]. When the problem with timing is considered (the prescribed angular positions of the active link are assigned to the precision points), the solution exists when at most five precision points are prescribed [15]. Irrespective of whether with or without timing a synthesis problem with three free choices is considered, only numerical methods have been worked out. In the present paper the problem with timing, with three conditions for positions and velocities, is dealt with. Moreover, this problem differs from the classical path synthesis problem in that the radial distances and radial velocities – not precision points nor absolute velocities – are prescribed. Newton iteration method is the most frequent mathematical method utilised in order to solve nonlinear equations. Nevertheless, the elimination methods (the techniques of numerical algebraic geometry), which are primarily based on homotopy methods, appeared to be most effective. Recently, polynomial continuation is being developed to deal with polynomial systems that may have higher dimensional solution sets, such as curves, surfaces, and so on [26]. These methods, however, require specialized numerical packages [25].

To solve the problem formulated in the present paper and find the set of approximate solutions the domain is searched through. An algorithm is proposed and described in the next subsection, in which 6 angular design parameters are simultaneously searched for. The finite ranges, from $-\pi$ to π, encompass all the domain, and no free choices are required, though, three of the angles can be prescribed (free chosen).

2.2. Solution algorithm

The algorithm worked out for the purposes of the method is referred to as 6DV2S (six design variables two steps). It allows one to determine the approximate solutions of Eqs. (12)–(15) in the specified domain and for the prescribed accuracy.

The input data, preliminary computations and constraints are as follows:

- The input data are: the coefficient of the spring stiffness, the minimum spring extension, the torque exerted on the disc, the relative angular positions of the disc (active link) in the balance positions (equilibrium): k, $u_3 = u_{\min}$, M_{E}, $\Delta\theta_{12}$, $\Delta\theta_{13}$. On the basis of the input data, spring extensions u_1, u_2 as well as their derivatives, $u'(0)$, $u'(\Delta\theta_{12})$, and $u'(\Delta\theta_{13})$ are computed from Eqs. (3) and (5).
- a, b, c, d are the lengths of the active link, coupler, passive link and immovable link, respectively. To ensure a reasonable proportion between the maximum $l_{\max} = \max(a,\ b,\ c,\ d)$ and minimum $l_{\min} = \min(a,\ b,\ c,\ d)$ dimensions, the upper limit w_1 for $\dfrac{l_{\max}}{l_{\min}}$ is prescribed.
- The acceptable value of the solution error is denoted as ε.
- The error is increased by w_2 when the Grashof conditions are not met.
- Two empty sets: X, E_R are defined.

The algorithm is divided into two parts.

Part I – Algorithm 6DV2S_I: The auxiliary mechanism is processed and the approximate solutions with the method error less than ε are searched for and written to set X.

I.1. γ_1, β_1 and λ_1 are set to zero. The unknowns are the initial positions of the links: $\boldsymbol{x}$, $\boldsymbol{a}$, $\boldsymbol{r}$, $\boldsymbol{y}$, $\boldsymbol{c}$, $\boldsymbol{R}$ as well as the angular positions of the links in the second and third balance positions. These angles are written in the form of a list $\chi = \{\gamma_2, \beta_2, \lambda_2, \gamma_3, \beta_3, \lambda_3\}$. We extract also a sublist $\chi_S = \{\gamma_2, \beta_2, \gamma_3, \beta_3\}$.

I.2. The set of linear equations (12) of complex variables is solved with respect to: $\boldsymbol{a}(\chi_S), \boldsymbol{x}(\chi_S), \boldsymbol{r}(\chi_S)$.

I.3. These solutions are substituted into equations (13).

The real and imaginary parts of Eqs. (13) are set to 0 in order to determine the rates of changes of angles with respect to θ_1: $\beta_1'(\chi_S)$ and $\gamma_1'(\chi_S)$ (from the first of Eqs. (13), i.e. $j = 1$), $\beta_2'(\chi_S)$ and $\gamma_2'(\chi_S)$ ($j = 2$), $\beta_3'(\chi_S)$ and $\gamma_3'(\chi_S)$ ($j = 3$).

I.4. The solutions of Eqs. (12): $\boldsymbol{a}(\chi_S)$, $\boldsymbol{x}(\chi_S)$, $\boldsymbol{r}(\chi_S)$ are substituted into Eqs. (14). The set of linear equations (14) of complex variables is solved with respect to: $\boldsymbol{c}(\chi), \boldsymbol{y}(\chi), \boldsymbol{R}(\chi)$.

I.5. The solutions of Eqs. (12)–(14): $\boldsymbol{a}(\chi_S)$, $\boldsymbol{x}(\chi_S)$, $\boldsymbol{r}(\chi_S)$, $\boldsymbol{c}(\chi)$, $\boldsymbol{y}(\chi)$, $\boldsymbol{R}(\chi)$, $\beta_1'(\chi_S)$, $\gamma_1'(\chi_S)$, $\beta_2'(\chi_S)$, $\gamma_2'(\chi_S)$, $\beta_3'(\chi_S)$, $\gamma_3'(\chi_S)$ are substituted into equations (15), and subsequently $\lambda_j' = \lambda_j'(\chi)$ for each $j = 1, 2, 3$ are determined, and real and imaginary parts are extracted $\lambda_j' = \mathrm{Re}(\lambda_j') + \mathrm{i}\,\mathrm{Im}(\lambda_j')$.

I.6. For an exact solution, the rate of relative change of angle λ with respect to θ_1 is a real number, therefore $\gamma_2, \beta_2, \lambda_2, \gamma_3, \beta_3, \lambda_3$ are searched for that satisfy the following set of equations:

$$\mathrm{Im}\left(\lambda_j'\right) = 0, \quad j = 1, 2, 3. \tag{16}$$

I.7. Three Eqs. (16) form a set of nonlinear algebraic equations, in which the unknown angles are the arguments of trigonometric functions. That is why the subdomain: $[\gamma_{2S}, \gamma_{2E}] \times [\beta_{2S}, \beta_{2E}] \times [\lambda_{2S}, \lambda_{2E}] \times [\gamma_{3S}, \gamma_{3E}] \times [\beta_{3S}, \beta_{3E}] \times [\lambda_{3S}, \lambda_{3E}]$ of domain $[-\pi, \pi]^6$ is searched for to find approximate solutions of Eqs. (16). The solution error is defined as

$$E(\chi) = \max_{j=1,2,3} \left|\mathrm{Im}(\lambda_j')\right|. \tag{17}$$

With the prescribed angles intervals and angles increments $\Delta\beta$, $\Delta\gamma$ and $\Delta\lambda$, the computations in the six loops are executed:

For $\gamma_2 = \gamma_{2S}$ to γ_{2E}, with step $\Delta\gamma$ do
  $\beta_2 = \beta_{2S}$ to β_{2E}, with step $\Delta\beta$ do
    For $\lambda_2 = \lambda_{2S}$ to λ_{2E}, with step $\Delta\lambda$ do
      For $\gamma_3 = \gamma_{3S}$ to γ_{3E}, with step $\Delta\gamma$ do
        For $\beta_3 = \beta_{3S}$ to β_{3E}, with step $\Delta\beta$ do
          For $\lambda_3 = \lambda_{3S}$ to λ_{3E}, with step $\Delta\lambda$ do
            Compute: $E(\chi)$.

If $E \leqslant \varepsilon$, then list χ is added to set of the solutions: $\mathrm{X} := \mathrm{X} \cup \chi$. The value of the error for this solution is also written, in set E_R.

I.8. Save the results to the disc and finish part I of the algorithm.

Herein, the brief discussion on the conditions (16) is required. λ'_j are real numbers for precise solutions, i.e., for the solutions that have physical meaning. The imaginary part of λ'_j should be zero for precise solutions, and it will be nearly zero for candidates for approximate solutions. Then, imaginary part of λ'_j is the magnitude of the solution error. The deviation from a real number may be also a consequence of floating point arithmetic. This means that if the last three equations (15) cannot be precisely met for any real angular velocities λ'_j, the geometry described by complex numbers $\boldsymbol{a}, \boldsymbol{x}, \boldsymbol{r}, \boldsymbol{d}, \boldsymbol{c}, \boldsymbol{R}$ fails to define the mechanism being an exact solution of the problem.

We note also that the list of six angular parameters χ only is a complete representation of the auxiliary mechanism, and in consequence, of the four-bar linkage with point E. One can reproduce the four-bar linkage (with point E) on the basis of these angles, which is realized by the second part of the algorithm. A solution χ from set X is evaluated in terms of the subsequent criteria (constraints). It should be emphasized that these criteria can be defined at the further stage of the analysis and can also be modified and adjusted to the current needs.

Part II – Algorithm 6DV2S_II: Processing of set X. Determination of the four-bar linkage geometry and verification of geometric constraints.

II.1. Select a solution $\chi_j \in \mathrm{X}$, $j = 1, \ldots, N$, where N is the number of solutions with error E_j (17) less than ε. The angles from χ_j are substituted into equations for $\boldsymbol{a}(\chi_\mathrm{S}), \boldsymbol{x}(\chi_\mathrm{S}), \boldsymbol{r}(\chi_\mathrm{S}), \boldsymbol{c}(\chi), \boldsymbol{y}(\chi), \boldsymbol{R}(\chi)$ determined in steps (I.2) and (I.4). The numbers $\boldsymbol{x}, \boldsymbol{a}, \boldsymbol{r}, \boldsymbol{y}, \boldsymbol{c}, \boldsymbol{R}$ represent the position of the four-bar linkage corresponding to the spring extension $u = u_1$. This position defines fully the mechanism. In order not to transform the solutions, the coordinate systems for the four bar linkage (Fig. 7) and auxiliary mechanism (Fig. 5) are parallel to each other with abscissa axis parallel to segment ED_1 and the ordinate axis perpendicular to ED_1. The only difference is that the origin is at point O_1 (Fig. 7), not at point E (Fig. 5).

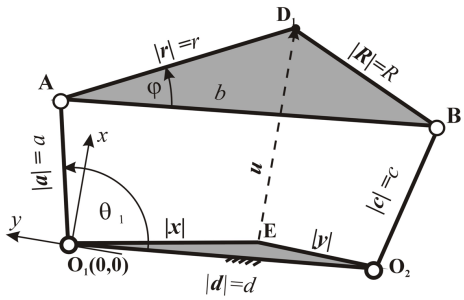

Fig. 7. The geometrical illustration for determination of the four-bar linkage in the first equilibrium position from auxiliary mechanism

Having obtained the auxiliary mechanism, the dimensions and joints coordinates of the four-bar linkage are determined:

- the coordinates of ground pivots O_1, O_2 and of point E:

$$O_1(0,0),\ O_2\left(\mathrm{Re}(\boldsymbol{y}-\boldsymbol{x}),\ \mathrm{Im}(\boldsymbol{y}-\boldsymbol{x})\right),\ E\left(-\mathrm{Re}(\boldsymbol{x}),\ -\mathrm{Im}(\boldsymbol{x})\right). \tag{18}$$

- the lengths of: ground link, arm AB of the coupler, input link O_1A and output link O_2B, respectively:

$$d = |\boldsymbol{y}-\boldsymbol{x}|, \quad b = |\boldsymbol{r}+\boldsymbol{R}|, \quad a = |\boldsymbol{a}|, \quad c = |\boldsymbol{c}|. \tag{19}$$

Angle θ_1, that defines the angular positions of link O_1A, is measured anticlockwise from the immovable segment O_1O_2. The angular position of the active link for $u = u_1$: θ_{11} is computed as the angle between vectors defined by complex numbers $\boldsymbol{a}$ and $\boldsymbol{d} = y - x$:

$$\theta_{11} = \pm \arccos\left(\frac{\mathrm{Re}(\boldsymbol{a})\,\mathrm{Re}(\boldsymbol{d}) + \mathrm{Im}(\boldsymbol{a})\,\mathrm{Im}(\boldsymbol{d})}{|\boldsymbol{a}|\,|\boldsymbol{d}|}\right). \tag{20}$$

One has to verify both signs to choose a proper one. Angle ϕ is measured anticlockwise between arms AB and AD of the coupler, and it is the angle between vectors defined by complex numbers $\boldsymbol{b}$ and $\boldsymbol{r}$. It must be manually specified which of the two four-bar linkage configurations realizes the desired motions.

II.2. The verification of geometric constraints.

II.2.A. Verification whether all the prescribed equilibrium positions are realized by the same four-bar linkage configuration (rejection of the cases with branch defects). The sign of the vector product ($\mathbf{AB}\times\mathbf{AO_2}$) must be the same for all three balance positions. When this condition is not met, the solution is rejected (removed from set X), and the algorithm returns to step II.I.

II.2.B. If $\dfrac{l_{\max}}{l_{\min}} \geqslant w_1$, then increase the solution error $E_j := E_j + \mu w_1$. By comparing the orders of magnitude for error E (17) and w_1, it was taken that $\mu = 10^{-4}$ (the value was established after performing preliminary simulations).

II.2.C. Grashof conditions are checked. If $2(l_{\max} + l_{\min}) > a + b + c + d$ or ($2(l_{\max} + l_{\min}) < a + b + c + d$ and ($l_{\min} = b$ or $l_{\min} = c$)), then $E_j := E_j + w_2$.

In general, it is not necessary for the active link to make a full revolution. Therefore, if the Grashof conditions are not imposed, one needs to verify whether a continuous active link rotation through angular positions θ_{11}, θ_{12} and θ_{13} is possible.

II.3. Determination of the direct error of balancing. The error (17) is not a direct measure of the balancing inaccuracy at the prescribed positions. To define the direct value of the error, the balancing torque acting on the disc, produced by the spring extended by $|\mathrm{DE}| = u(\theta_1)$, is computed:

$$M_t = -\frac{\mathrm{d}}{\mathrm{d}\theta_1}\left(\frac{1}{2}ku\,(\theta_1)^2\right). \tag{21}$$

This torque is to balance the external torque M_{E}. Therefore, the direct error of the method is expressed as the average value of the unbalanced torques in the three prescribed positions:

$$\Delta M = \sum_{i=1}^{3} \frac{|M_{\mathrm{E}} - M_t\,(\theta_{1i})|}{3}. \tag{22}$$

II.4. If the solution is not satisfactory, repeat steps II.1–II.3 for a subsequent solution $\chi \in \mathrm{X}$. The evaluation of the solution fitness is based on the subjective estimation.

Due to the kinematic inversion, this technique does not require the determination of radial components of the relative velocity of point D with respect to point E. The proposed algorithm simplifies the formulation of the objective function, which does not contain two physically different quantities (distance u and velocity $\mathrm{d}u/\mathrm{d}\theta_1$). Let us recall that even though the optimization consists in the minimization of the two terms: the deviation of distance |DE| from the prescribed value u: |DE| – u, and the deviation of the obtained value of the radial component of point D velocity in the relative motion with respect to E from the prescribed value, the solution fitness is expressed by the deviation of the angular velocity of a mechanism link from a real number.

Computations are performed in *Mathematica 10*. The software makes it possible to carry out symbolic transformations of complex linear equations up to step I.6. The last equations (16) are non-linear trigonometric equations. That is why the domain is discretised and the values of error (17) in the nodes of the domain are computed using the systematic search method. In general, the number of solutions may be infinite. The number is finite when the problem is to find the solutions meeting geometric constraints, e.g., the magnitude of the links, transmission angle range, etc. The efficiency of the method has been discussed on the basis of many algorithm runs for various parameters values.

3. Numerical solutions

For all the cases it is assumed that:

- The external torque $M_{\mathrm{E}} = 156.96$ Nm.
- The permitted ratio of the maximum and minimum link length $w_1 = 10$. If w_1 is greater than 10, the solution is rejected.
- Parameter $w_2 = 0$ (the Grashof conditions are not imposed).

The algorithm was run for various spring stiffness coefficients, minimum spring extensions and the angular increments corresponding to the input link (disc) rotations from the first to second balance positions – $\Delta\theta_{12}$, and from the first to third balance positions – $\Delta\theta_{13}$.

The chosen solutions for five cases, with the input data given in Table 1, are presented. The most compact form of the illustrative results for each case is given in

Table 2, since the mechanism geometries can be easily determined by substituting these numbers into Eqs. (18)–(19).

Table 1. Input data for the numerical solutions

Case	k [N/m]	$u_{\min} = u_3$ [m]	$\Delta\theta_{12}$	$\Delta\theta_{13}$
I.1.A	$5 \cdot 10^3$	0.2	$3\pi/8$	$3\pi/4$
II.1.A	10^4	0.05	$\pi/4$	$7\pi/8$
III.1.A	$4 \cdot 10^4$	0.1	$\pi/5$	$\pi/2$
III.1.B			$\pi/2$	$3\pi/2$
III.2.A		0.15	$\pi/3$	$2\pi/3$

Table 2. The exemplary solutions

Case	Solution
I.1.A	$\boldsymbol{a} = 0.01569 + 0.270248\mathrm{i}$, $\boldsymbol{R} = 0.144847 + 0.1106\mathrm{i}$, $\boldsymbol{r} = -0.42755 - 0.32508\mathrm{i}$, $\boldsymbol{x} = 0.84537 + 0.05483\mathrm{i}$, $\boldsymbol{c} = 1.36195 - 1.20043\mathrm{i}$, $\boldsymbol{y} = -0.78359 + 1.31103\mathrm{i}$
II.1.A	$\boldsymbol{a} = 0.14462 + 0.12835\mathrm{i}$, $\boldsymbol{R} = -0.08795 - 0.25607\mathrm{i}$, $\boldsymbol{r} = 0.12784 - 0.14961\mathrm{i}$, $\boldsymbol{x} = 0.02552 + 0.02125\mathrm{i}$, $\boldsymbol{c} = 0.34393 - 0.16205\mathrm{i}$, $\boldsymbol{y} = -0.13389 - 0.09402\mathrm{i}$.
III.1.A	$\boldsymbol{a} = -0.014299 - 0.011599\mathrm{i}$, $\boldsymbol{R} = -0.00882 + 0.16443\mathrm{i}$, $\boldsymbol{r} = 0.081876 - 0.16389\mathrm{i}$, $\boldsymbol{x} = 0.081847 + 0.17549\mathrm{i}$, $\boldsymbol{c} = -0.12141 - 0.04614\mathrm{i}$, $\boldsymbol{y} = 0.262013 + 0.210572\mathrm{i}$.
III.1.B	$\boldsymbol{a} = 0.012477 - 0.0766896\mathrm{i}$, $\boldsymbol{R} = 0.0862681 + 0.445733\mathrm{i}$, $\boldsymbol{r} = 0.120286 + 0.199395\mathrm{i}$, $\boldsymbol{x} = 0.0839926 - 0.122705\mathrm{i}$, $\boldsymbol{c} = 0.384869 + 0.798724\mathrm{i}$, $\boldsymbol{y} = -0.081846 - 0.352991\mathrm{i}$.
III.2.A	$\boldsymbol{a} = 0.049708 - 0.00697\mathrm{i}$, $\boldsymbol{R} = -0.016777 + 0.030879\mathrm{i}$, $\boldsymbol{r} = 0.000159 + 0.035569\mathrm{i}$, $\boldsymbol{x} = 0.147457 - 0.0286\mathrm{i}$, $\boldsymbol{c} = -0.134069 - 0.154618\mathrm{i}$, $\boldsymbol{y} = 0.314616 + 0.185497\mathrm{i}$.

Case I.1.A

On this basis of the input data (Table 1) the following parameters are computed from Eqs. (3) and (5) (the linear dimensions are expressed in [m], velocities are in [m/rad], angles are in [rad]): $u_{\max} = u_1 = 0.43351$, $u_2 = 0.33759$, $u_{\min} = u_3 = 0.2$, $v_1 = u_1' = -0.07241$, $v_2 = u_2' = -0.09299$, $v_3 = u_3' = -0.15696$.

As a result of the execution of algorithm **6DV2S_I** – processing of the auxiliary mechanism – the set of solutions was obtained, and the solutions were verified to reject the ones with branch defects. The exemplary solution is presented: $\beta_2 = 0.94984$, $\beta_3 = 0.43197$, $\gamma_2 = 0.75104$, $\gamma_3 = 1.00138$, $\lambda_2 = 0.58905$, $\lambda_3 = 0.785392$.

Having run part II of the algorithm – determination of the four-bar linkage – one gets $\boldsymbol{a}, \boldsymbol{r}, \boldsymbol{R}, \boldsymbol{x}, \boldsymbol{c}, \boldsymbol{y}$ (Table 2), and further: $a = 0.2707$, $b = 0.35486$, $c = 1.81547$, $d = 2.05708$, $r = 0.5371$, $\theta_{11} = -0.97188$, $\phi = 0.00106$, $\mathrm{O}_1(0, 0)$, $\mathrm{O}_2(-1.629, 1.256)$, $E(-0.845, -0.055)$. The average torque error (22) is $\Delta M = 2.091$ Nm and method error $E = 7.88835 \cdot 10^{-4}$ (the maximum value of the imaginary part of the rate of change of λ in function of θ_1 in the balance positions is equal to E, which is about 1% of the real part). The scheme of the mechanism with the coupler point D

trajectory is presented in Fig. 8, with points D_1, D_2 and D_3, such that $|D_iE| \approx u_i$. The resultant torque M is presented in Fig. 9. The prescribed equilibrium positions are marked with dots. The spring extension and the rate of spring extension with respect to the active link angle are shown in Figs 10 and 11. The dots stand for the values that guarantee the exactly balanced mechanism in the prescribed positions. The dotted lines in Figs 10 and 11 are the theoretical functions for the spring extension and the rate of the spring extension that guarantee continuous balancing when passing from the first position to the last one.

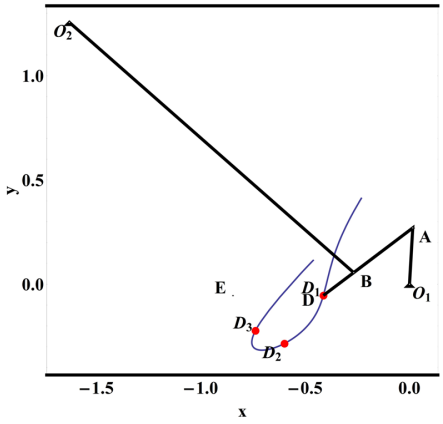

Fig. 8. The mechanism in case I.A.1

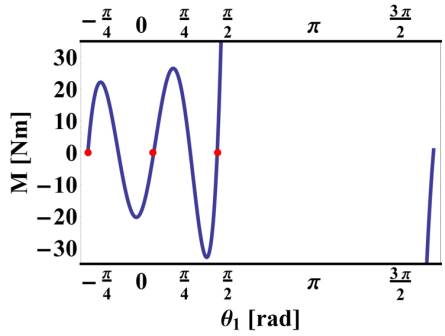

Fig. 9. The resultant torque on the input link in case I.A.1 with the prescribed balance positions (dots)

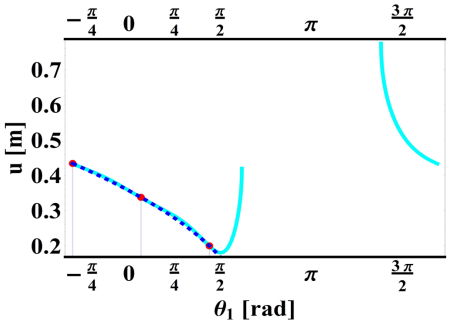

Fig. 10. The spring extension in case I.A.1 with the extensions required for balancing (dots)

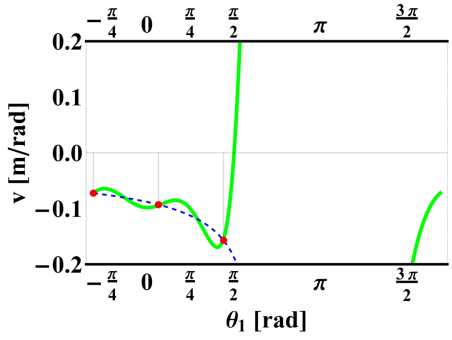

Fig. 11. The rate of the spring extension in case I.A.1 with the rate required for balancing (dots)

We can notice that the three equilibrium positions are stable. We aim at minimizing the resultant torque M, i.e., the difference between the theoretical balancing torque produced by the spring (21) and the external, input torque in the prescribed

positions $M = M_E - M_t(\theta_1)$. As can be seen in Fig. 9, the resultant torque direction changes in the vicinity of the equilibrium positions. On the left hand side of a required equilibrium position, the resultant torque is negative (the clockwise external torque is less than the anticlockwise torque produced by the spring), then acts anticlockwise and rotates the disc anticlockwise (to the right hand side of the abscissa axis) to the equilibrium position. On the right hand side of an equilibrium position, the resultant torque is positive (the clockwise external torque is greater than the anticlockwise torque produced by the spring), then acts clockwise and rotates the disc clockwise (to the left hand side of the abscissa axis) to the equilibrium position. The stable equilibrium positions are separated by unstable equilibrium positions, as six equilibrium positions occur in the allowed range of motion.

Case II.1.A

On this basis the input data, the following parameters are computed: $u_{\max} = u_1 = 0.297982$, $u_2 = 0.2532549$, $u_{\min} = u_3 = 0.05$, $u_1' = -0.05267$, $u_2' = -0.062$, $u_3' = -0.31392$. As a result of the execution of algorithm **6DV2S_I** the set of solutions was obtained, and an exemplary solution is defined by: $\beta_2 = -0.11562$, $\beta_3 = 0.14$, $\gamma_2 = -0.54978$, $\gamma_3 = -1.18956$, $\lambda_2 = -0.2227$, $\lambda_3 = -0.7654$. Having run part II of the algorithm (Table 2), one obtains: $a = 0.19337$, $b = 0.40764$, $c = 0.38019$, $d = 0.19673$, $r = 0.19679$, $\theta_{11} = -3.04182$, $\phi = 0.60907$, $O_2(-0.159, -0.115)$, $E(-0.0255, -0.021)$, $\Delta M = 0.6813$ Nm, $E = 18.80181 \cdot 10^{-4}$. The solutions are presented in Figs 12, 13.

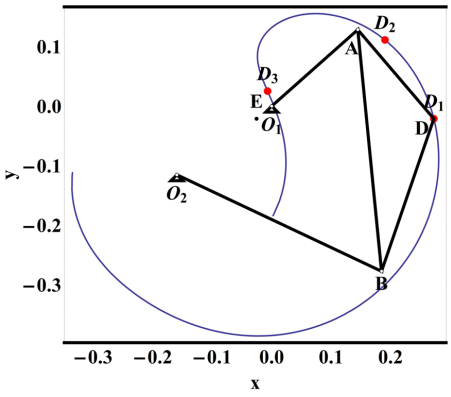

Fig. 12. The mechanism in case II.1.A

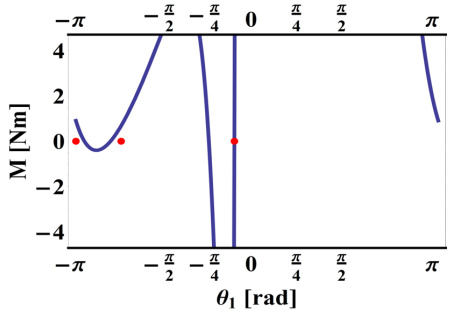

Fig. 13. The resultant torque on the input link in case II.1.A with the prescribed balanced positions

Case III.1.A

The exemplary solution, for which $\Delta M = 2.6728$ Nm and $E = 9.16 \cdot 10^{-4}$, is presented in Figs 14, 15. It is visible that, as opposed to the previous solutions, the mechanism meets the Grashof conditions.

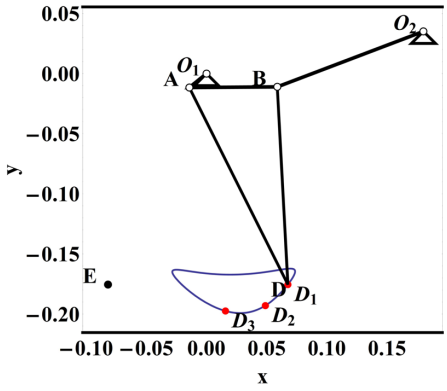

Fig. 14. The mechanism in case III.1.A

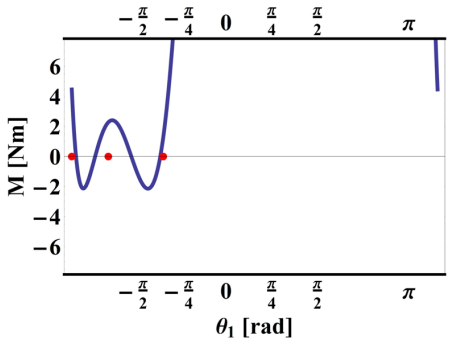

Fig. 15. The resultant torque on the input link in case III.1.A with the prescribed balanced positions

Case III.1.B

Compared to case III.I.A, the angular increments only were changed (increased). The solution, with $\Delta M = 2.073$ Nm, and $E = 55.945 \cdot 10^{-4}$, is presented in Figs 16, 17.

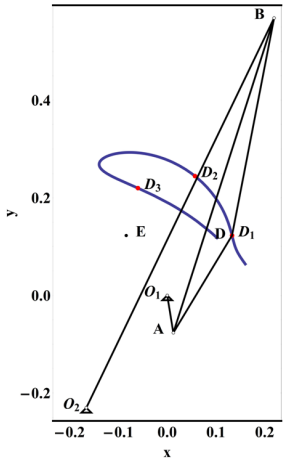

Fig. 16. The mechanism in case III.1.B

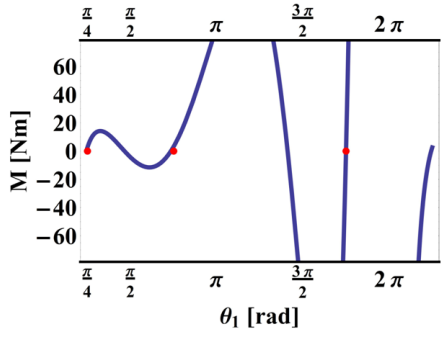

Fig. 17. The resultant torque on the input link in case III.1.B with the prescribed balanced positions

Case III.2.A

In this case the spring stiffness is equal to that in cases III.x.x, $u_{\min}$ and the angular increments were changed. The exemplary solution, for which $\Delta M = 1.128$ Nm, and $E = 36.658 \cdot 10^{-4}$, is presented in Figs 18, 19. We can conclude that the mechanism size limitations significantly affect the error value. One can

observe a tendency that the mechanisms having very small method errors (and simultaneously holding the Grashof conditions) are characterized by a high ratio of the maximum dimension to the minimum one.

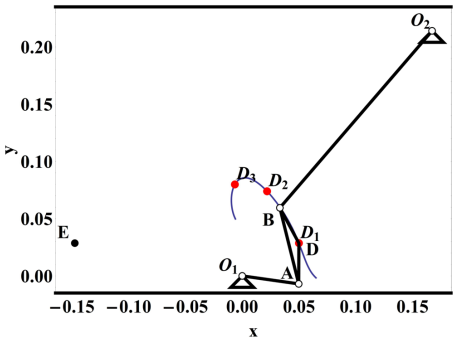

Fig. 18. The mechanism in case III.2.A in the third balanced position

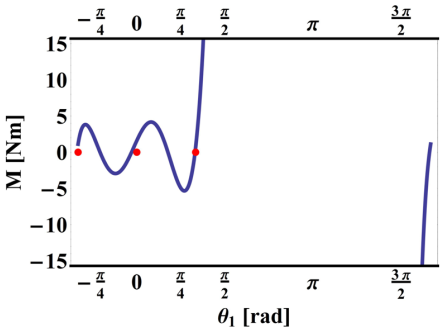

Fig. 19. The resultant torque on the input link in case III.2.A with the prescribed balanced positions

The resultant torques obtained using the energetic approach were compared to the torques obtained using the classical equilibrium equations written for all the links. Such an approach is presented in paper [27] to balance a system over a continuous range of motion. The results are identical.

Supplementary materials are available as the data stored in repository *Mendeley Data* [28]. SolutionData.doc contains the exemplary solutions of algorithm 6DV2S_I. The notebook 4Bar3Points_6DV2S_II_A.nb created in Wolfram Mathematica 8.0 is the code of algorithm 6DV2S_II for determining the mechanism dimensions from the output data of algorithm 6DV2S_I and for the results visualization. The zip file *SupplFigs* contains the figures of the spring extensions and the rates of the spring extensions for all the cases except for I.A.1. The name of the figure addresses the adequate case.

4. Conclusions

For the purpose of torque balancing in the three prescribed angular positions, the four-bar linkage with a spring was proposed, and the new problem of the mechanism synthesis was formulated. A general method was developed for determining the four-bar linkage with the defined three conditions concerning the position of coupler point and three conditions concerning the velocity components of this point. The method description is based on the linear algebraic equations and, not earlier than in the last step, it is required to apply a numerical technique in order to find the approximate solutions.

The presented approach, in particular, has the following advantages:

- A new problem of discrete position balancing of linkages is considered and the solution method is worked out for the balancing system composed of the four-bar linkage and spring. The method works for three prescribed positions. After slight modification, the method can be applied to balance both a torque and input force acting on any member of the system.
- Kinematic inversion provided the simpler form of the equations for radial component of the spring-coupler point. There is no derivative term resulting from the motion direction change of ED (rotary lifting motion) in the four-bar linkage.
- The set of virtual solutions is obtained from which the user may select those satisfying the additional constraints. Double step approach allows one to determine the sets of solutions that can be processed in terms of different constraints.
- A solution defines the initial mechanism position, which reduces the number of designed variables. By means of six angles: $\chi = \{\gamma_2, \beta_2, \lambda_2, \gamma_3, \beta_3, \lambda_3\}$ the four-bar linkage and the coordinates of ground point E were described. Hence, the number of variables needed for recording the solution is minimized and it is 6 instead of 8. Algorithm 6DV2S_II presents the procedure of determining, firstly: $\boldsymbol{x}$, $\boldsymbol{a}$, $\boldsymbol{r}$, $\boldsymbol{y}$, $\boldsymbol{c}$, $\boldsymbol{R}$, and secondly, the six dimensions: a, b, c, d, r, x_E and two angles: ϕ and δ. Angles χ together with $\{\gamma_1, \beta_1, \lambda_1\} = \{0, 0, 0\}$ define, at the same time, unequivocally the three equilibrium positions.

One can indicate some drawbacks of the developed approach. Searching in a large set with the high density may be time-consuming. The limitation of the number of design variables sometimes may lead to unacceptable results. On the other hand, it is possible to apply an evolutionary algorithm in order to improve the solutions or to apply this algorithm directly as a method of determining the design variables. Notwithstanding the minor errors of the kinematic synthesis, there may be a high torque gradient at a equilibrium position. The problems of the solutions sensitivity to errors related to the imperfections of manufacturing (dimension deviations) and assembly as well as joint clearance require a separate and comprehensive research field supported with a plenty of analyses.

A. Appendix

Fig. A1 shows the geometrical construction of the first equilibrium position of the mechanism for case I.1.A. As shown in Fig. 5, complex numbers $\boldsymbol{a}$, $\boldsymbol{c}$, $\boldsymbol{R}$, $\boldsymbol{r}$, $\boldsymbol{x}$ and $\boldsymbol{y}$ computed by the algorithm represent the vectors. As a result the mechanism presented in Fig. 8 is obtained.

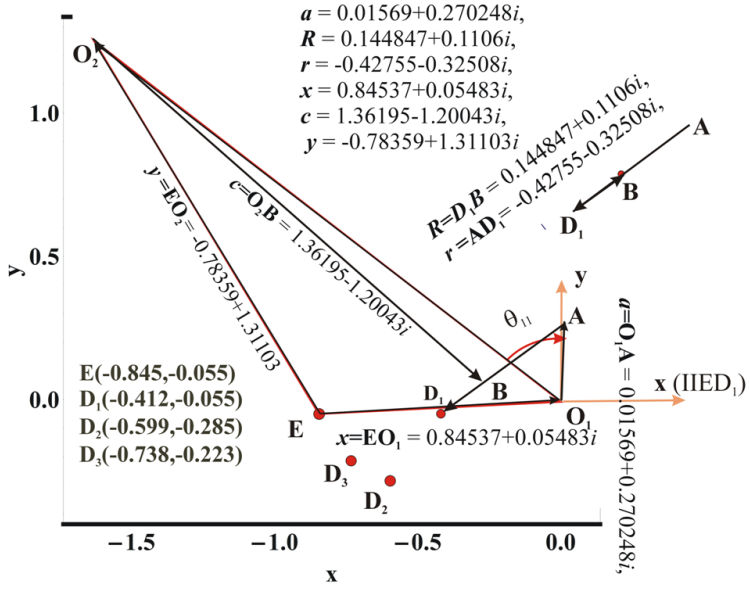

Fig. A1. The construction of the mechanism in the first equilibrium position (case I.1.A)

Acknowledgements

This work was supported by the Polish Ministry of Education and Science. The grant number 0612/SBAD/3588.

References

[1] V.H. Arakelian and S. Briot. *Balancing of Linkages and Robot Manipulators. Advanced Methods with Illustrative Examples*. Springer, 2015.

[2] P. Wang and Q. Xu. Design and modeling of constant-force mechanisms: A survey. *Mechanism and Machine Theory*, 119:1–21, 2018. doi: 10.1016/j.mechmachtheory.2017.08.017.

[3] V. Arakelian and M. Mkrtchyan. Design of scotch yoke mechanisms with balanced input torque. In *Proceedings of the ASME 2015 International Design Engineering Technical Conferences & Computers and Information in Engineering Conference IDETC/CIE 2015*, pages 1–5, Boston, Massachusetts, USA, 2–5 August, 2015. doi: 10.1115/DETC2015-46709.

[4] J.A. Franco, J.A. Gallego, and J.L. Herder. Static balancing of four-bar compliant mechanisms with torsion springs by exerting negative stiffness using linear spring at the instant center of rotation. *Journal of Mechanisms and Robotics*, 13(3):031010–13, 2021. doi: 10.1115/1.4050313.

[5] B. Demeulenaere and J. De Schutter. Input torque balancing using an inverted cam mechanism. *Journal of Mechanical Design*, 127(5):887–900, 2005. doi: 10.1115/1.1876452.

[6] D.A. Streit and E. Shin. Equilibrators for planar linkages. *Journal of Mechanical Design*, 115(3):604–611, 1993. doi: 10.1115/1.2919233.

[7] Y. Liu, D.P. Yu, and J. Yao. Design of an adjustable cam based constant force mechanism. *Mechanism and Machine Theory*, 103:85–97, 2016. doi: 10.1016/j.mechmachtheory.2016.04.014.

[8] J.L. Herder. Design of spring force compensation systems. *Mechanism and Machine Theory*, 33(1-2):151–161, 1998. doi: 10.1016/S0094-114X(97)00027-X.

[9] S.R. Deepak and G.K. Ananthasuresh. Static balancing of a four-bar linkage and its cognates. *Mechanism and Machine Theory*, 4:62–80, 2012. doi: 10.1016/j.mechmachtheory.2011.09.009.

[10] S. Perreault, P. Cardou, and C. Gosselin. Approximate static balancing of a planar parallel cable-driven mechanism based on four-bar linkages and springs. *Mechanism and Machine Theory*, 79:64–79, 2014. doi: 10.1016/j.mechmachtheory.2014.04.008.

[11] J. Buśkiewicz. The optimum distance function method and its application to the synthesis of a gravity balanced hoist. *Mechanism and Machine Theory*, 139:443–459, 2019. doi: 10.1016/j.mechmachtheory.2019.05.006.

[12] V.L. Nguyen. A design approach for gravity compensators using planar four-bar mechanisms and a linear spring. *Mechanism and Machine Theory*, 172:104770, 2022. doi: 10.1016/j.mechmachtheory.2022.104770.

[13] R. Barents, M. Schenk, W.D. van Dorsser, B.M. Wisse, and J.L. Herder. Spring-to-spring balancing as energy-free adjustment method in gravity equilibrators. *Journal of Mechanical Design*, 133(6):689–700, 2011. doi: 10.1115/DETC2009-86770.

[14] I. Simionescu and L. Ciupitu. The static balancing of the industrial robot arms, Part I: discrete balancing. *Mechanism and Machine Theory*, 35(9):1287–1298, 2001. doi: 10.1016/S0094-114X(99)00067-1.

[15] A.G. Erdman and G.N. Sandor. *Mechanism Design: Analysis and Synthesis*, Vol. 1, 4th ed., Prentice-Hall, Upper Saddle River, NJ, 2001.

[16] G.N. Sandor and A.G. Erdman. *Advanced Mechanism Design: Analysis and Synthesis*, Vol. 2, Prentice Hall, Englewood Cliffs, NJ, 1997.

[17] J.M. McCarthy and G.S. Soh. *Geometric Design of Linkages*, Vol. 11, Springer, New York, 2011.

[18] H. Kaustubh, J. Sonawale, and J.M. McCarthy. A design system for six-bar linkages integrated with a solid modeler. *Journal of Computing and Information Science in Engineering*, 15(4):041002, 2015. doi: 10.1115/1.4030940.

[19] J. Han and W. Liu. On the solution of eight-precision-point path synthesis of planar four-bar mechanisms based on the solution region methodology. *Journal of Mechanisms and Robotics*, 11(6):064504, 2019. doi: 10.1115/1.4044544.

[20] C.W. Wampler, A.P. Morgan, and A.J. Sommese. Complete solution of the nine-point path synthesis problem for four-bar linkages. *Journal of Mechanical Design*, 114(1):153–159, 1992. doi: 10.1115/1.2916909.

[21] W. Guo and X. Wang. Planar linkage mechanism design for bi-objective of trajectory and velocity. *J Beijing Univ Aero Astronautics*, 35(12):1483–1486, 2009.

[22] J. Han, W. Qian, and H. Zhao. Study on synthesis method of λ-formed 4-bar linkages approximating a straight line. *Mechanism and Machine Theory*, 44(1):57–65, 2009. doi: 10.1016/j.mechmachtheory.2008.02.011.

[23] J.E. Holte, T.R. Chase, and A.G. Erdman. Approximate velocities in mixed exact-approximate position synthesis of planar mechanisms. *Journal of Mechanical Design*, 123(3):388–394, 2001. doi: 10.1115/1.1370978.

[24] W.T. Lee and K. Russell. Developments in quantitative dimensional synthesis (1970–present): Four-bar path and function generation. *Inverse Problems in Science and Engineering*, 26(9):1280–1304, 2017. doi: 10.1080/17415977.2017.1396328.

[25] C. Wampler and A. Sommese, Numerical algebraic geometry and algebraic kinematics. *Acta Numerica*, 20:469–567, 2011. doi: 10.1017/S0962492911000067.

[26] D.A. Brake, J.D. Hauenstein, A.P. Murray, D.H. Myszka, and C.W. Wampler. The complete solution of alt-burmester synthesis problems for four-bar linkages. *Journal of Mechanisms and Robotics*, 8(4): 041018, 2016. doi: 10.1115/1.4033251.

[27] J. Buśkiewicz, 2019, Gravity balancing of a hoist by means of a four-bar linkage and spring. In: *Advances in Mechanism and Machine Science: Proceedings of the 15th IFToMM World Congress on Mechanism and Machine Science*, pages 1721–1730, Cracow, Poland, June, 2019. doi: 10.1007/978-3-030-20131-9_170.

[28] J. Buśkiewicz. Solution data, the code of algorithm 6dv2s_II in Mathematica wolfram 8.0 and pdf file of the code, the figures of the spring extensions and the rates of the spring extensions for all the cases. Mendeley Data, V3, 2022, https://data.mendeley.com/datasets/sb38dsw6vm/3.